Mon. Not. R. astr. Soc. (1981) **196**, 611–633

Multifrequency models for the cosmological evolution of extragalactic radio sources

J. A. Peacock* and S. F. Gull *Mullard Radio Astronomy Observatory, Cavendish Laboratory, Madingley Road, Cambridge CB3 0HE*

Received 1981 January 7; in original form 1980 November 19

Summary. This paper presents new models for the epoch dependence of the luminosity function of extragalactic radio sources. These models have been derived on the assumption that radio sources may be divided into two distinct populations: the extended steep-spectrum sources and the compact flat-spectrum sources. By using the correlation between luminosity and spectral index for the steep-spectrum sources, the luminosity functions defined at different frequencies may be related, allowing a single model to be tested against all available source counts, luminosity distributions and identification data. To obtain models that are consistent with the data, the luminosity functions for each of the two spectral classes are expressed as free series expansions in luminosity and redshift, and the expansion coefficients that yield the best-fitting models are found iteratively. Different expansion forms are considered in order to estimate the uncertainty in the luminosity function; it is found that, in most areas of the P–z plane, the luminosity function is poorly defined and a variety of evolutionary histories are possible. Within the regions which are well defined by the redshift information from bright-source samples, however, both the steep-spectrum and flat-spectrum sources appear to behave similarly: powerful sources of either type undergo strong evolution.

1 Introduction

This paper is concerned with the changes of the radio-source population that occur with cosmological epoch. That such evolution is a necessity has been known since the production of the first reliable source counts; these were inconsistent with any model of the Universe in which the comoving density of radio sources was fixed. As optical identifications and redshifts became available for samples of bright sources, it was apparent from the wide range of luminosities present that the observed rapid convergence of the source counts towards low flux densities could only be explained if the powerful sources alone changed their comoving densities (Longair 1966). In order to provide a quantitative description of this evolution, it is usual to consider the change with epoch of the Radio Luminosity Function (hereafter RLF), which is defined to be the number of sources per unit comoving volume per

* Present address: Royal Observatory, Blackford Hill, Edinburgh EH9 3HJ, Scotland.

unit interval of $\log_{10}(P)$ (where P is the luminosity in $\mathrm{W\,Hz^{-1}\,sr^{-1}}$). The RLF, $\rho(P, z)$, is often factorized as follows:

$$\rho(P, z) = \rho_0(P)\, E(P, z),$$

where ρ_0 is the RLF at the present epoch, and the function E is called the evolution function. This latter is the physically important quantity; it contains information about the creation of radio sources and their subsequent history. The usefulness of considering only the RLF rests on the fact that the luminosity of a source may often be taken as an indication of its physical type, since many properties (e.g. radio morphology, optical identification, radio and optical spectrum) correlate well with luminosity. However, we must also allow for the fact that radio sources may be divided into two distinct populations: the extended, steep-spectrum sources and the compact, flat-spectrum sources. The former are those familiar from low-frequency surveys, with the majority of their emission originating in structure of scale $\gtrsim 1$ kpc, whereas the latter are dominated by an unresolved high-brightness component, which may be of scale ~ 10 pc. These compact sources are usually identified with quasars, and are found predominantly in high-frequency surveys. The fact that the emission occurs on such different scales in these two classes suggests that they should be treated as physically distinct. The usual way in which these objects are distinguished is by their radio spectra; extended sources generally have power-law spectra with high-frequency spectral indices > 0.5 (where $S \propto \nu^{-\alpha}$), whereas the spectra of compact sources are usually affected by synchrotron self-absorption, leading to spectral indices < 0.5 (see e.g. Wall 1975). This division at $\alpha = 0.5$ is crude, but does appear to be effective in separating compact from extended sources in most cases (see e.g. Peacock & Wall 1981). In the remainder of this paper, we shall use the terms steep-spectrum and flat-spectrum to mean $\alpha \geqslant 0.5$ or $\alpha < 0.5$ respectively.

Many attempts have been made to find models that describe the evolution of the RLF; the more successful are described in Section 2. These analyses have served to define the broad features of the evolutionary behaviour of extragalactic radio sources. For the steep-spectrum sources, strong differential evolution as a function of luminosity has been confirmed, although no conclusions as to the necessity for a redshift cutoff have been reached. On the other hand, very little has been learned about the flat-spectrum sources, simply because the data on these objects were very poor by comparison with those available on the steep-spectrum sources. This situation has improved recently: in particular the 5-GHz source counts (Kellermann 1980) and the 2.7-GHz luminosity distributions (Peacock & Wall 1981) are now defined with much greater precision, and the time is ripe for a fresh approach to the construction of evolution models.

The work described in this paper has two main purposes:

(a) To find a modelling procedure which can account for the observational data at all frequencies (incorporating the recent data on flat-spectrum sources). This procedure should be able to incorporate any specified geometry.

(b) To consider to what extent the models are unambiguously constrained by the data. In particular, we wish to discover whether the data provide any evidence for the two most common features of evolution models: differential evolution and redshift cut-offs.

We shall consider the Universe to have the geometry of the Friedmann–Robertson–Walker models of General Relativity. A Hubble constant of $50\,\mathrm{km\,s^{-1}\,Mpc^{-1}}$ will be assumed (where results of other workers are quoted, these have been converted to be consistent with this value) and, to indicate the dependence on geometry, we shall derive solutions for both the 'empty Universe' ($q_0 = 0$) and the 'Einstein–de Sitter Universe' ($q_0 = 0.5$). Our technique may be extended immediately to any other isotropic geometry.

2 Previous models of evolution

Recent attempts to find the RLF from the observational data include those by Grueff & Vigotti (1977), Robertson (1978, 1980) and Wall, Pearson & Longair (1980, 1981). The models of Wall *et al.* (1980; henceforth WPL) were based on data taken at 408 MHz only. WPL adopted a procedure in which the powerful sources were all assumed to have the same evolution – either $E \propto (1+z)^n$ (power-law evolution) or $E \propto \exp(m\tau)$ (exponential evolution, where τ is the normalized 'look-back' time, $\tau = 1 - t/t_0$). This evolution was assumed to 'turn on' over a range of 408-MHz luminosities lying between 10^{25} and $10^{27}\,\mathrm{W\,Hz^{-1}\,sr^{-1}}$. The parameters n and m, and the critical luminosity range, were adjusted until the best fit was found to the source counts and to a luminosity distribution for sources brighter than 10 Jy. The exponential models were successful, but the power-law models could not reproduce the data precisely, although good qualitative agreement was obtained, provided a redshift cut-off at $z \simeq 3$ was introduced.

Robertson also assumed that all powerful sources evolved in the same way, again using a range of 'turn-on' luminosities. The evolution function in this case, however, was found in a free-form manner, sampling E at 100 different points in redshift and allowing each point to vary independently until convergence was achieved. This procedure yielded a single evolution function for a given geometry, although only $q_0 = 0.5$ was investigated. The disadvantages with this method are two-fold: first, the function produced may not be smooth; secondly, this process yields little information as to the range of E allowed by the data. It should also be emphasized that this approach is not truly free-form, because of the way in which the sampling of E is carried out. Robertson chose to sample E at equal intervals in $\log(z)$, which corresponds to the tacit assumption that E should be a smooth function in this coordinate frame (see Section 3).

The approach of Grueff & Vigotti was a semi-physical one, involving a number of *ad hoc* assumptions about the nature of the evolution. In their picture, all radio sources were created at a redshift of 2.5 as quasars, and turned into radio galaxies of the same radio luminosity at a rate which depended on luminosity. The numbers of these radio galaxies were then assumed to decay at a different rate, again luminosity-dependent. These rates were adjusted to produce consistency with source counts and luminosity information derived from 408-MHz samples selected at 10 and 0.9 Jy. This approach has the advantage of dealing with the evolution of galaxies and quasars independently, the only one to do so, but the necessary assumptions are hard to test. For example, it is assumed that the sources with low luminosities at high redshifts are quasars, rather than the normal galaxies which constitute the lowest-luminosity sources at low redshifts. The problem, as with all the other approaches, is that preconceived ideas as to the form of the evolution are supplied, rather than allowing the data to specify which forms of evolution are allowed and which are not.

All these models were constructed by using samples of sources selected at 408 MHz only. Such samples are well known to consist largely of extended, steep-spectrum sources. As the survey frequency is raised, increasing numbers of compact, flat-spectrum sources are found (see e.g. Wall 1980). As discussed in Section 1, these are a physically distinct class of object and should, in principle, be allowed a different evolutionary behaviour. The two source-count analyses which attacked this problem were those of Kulkarni (1978) and Wall *et al.* (1981). Both divided the RLF into the steep-spectrum and flat-spectrum components, assumed one of the WPL models to apply for the steep-spectrum sources, and ascribed similar forms of evolution to the flat-spectrum sources. This allowed Wall *et al.* to fit source counts at 408 and 2700 MHz, and Kulkarni to fit source counts at 408 and 5000 MHz, but little was learned from these studies about the flat-spectrum sources, due to the inadequacy

of the luminosity data for these objects, and no attempts were made to re-optimize the evolution model for the steep-spectrum sources.

3 Relating RLFs at different frequencies

The use of a model RLF to obtain predictions for comparison with observational data may be described in terms of the luminosity–redshift (P–z) plane. For example, predicted source counts are obtained by constructing lines of constant flux density on the P–z plane, and integrating between two such lines the product of $\rho(P, z)$ and the corresponding volume element. In practice, we chose to carry out such calculations on a grid of points 100 square for each spectral type. The grids covered the range $P(2.7\,\mathrm{GHz})/(\mathrm{W\,Hz^{-1}\,sr^{-1}}) = 10^{20}$ to 10^{30} linearly in $\log(P)$, and the range $z = 0.01$ to 100 linearly in $\log(z)$. The sampling in $\log(z)$ is necessary so that the volume elements corresponding to the redshift increment at each gridpoint were of the same order. The first gridpoint in redshift accounted for all redshifts less than 0.01. The size 100×100 has been found useful in the past (see e.g. WPL), as it is sufficiently closely sampled to allow accurate values to be read from the grid without the necessity of interpolation.

To convert a model for the population of the P–z plane into predicted data, we must be able to find flux densities, i.e. we need to find $S(P, z)$. This depends both on the particular geometry adopted and also on the spectra of the objects involved. WPL assumed that the observed distribution of spectral indices could be modelled by taking all sources to have a spectral index of 0.75. This procedure is valid if the RLF thus derived is to be used at one frequency only. Since, for the majority of sources, $(1 + z)$ will be in the range 1–4, errors of 0.2–0.4 in α will not significantly move the lines of constant flux density with respect to the major features on the RLF. If it is desired to make predictions at different frequencies, however, then errors in the RLF and the way it is sampled will be important; although the errors in the RLF and in the sampling procedure cancel out at the defining frequency, this will not be the case at a different frequency. We see therefore that the WPL models may need modifying for two reasons: (i) the well-known existence of a correlation between luminosity and spectral index; and (ii) the possibility of separate evolution for the flat-spectrum sources. The existence of a spread of spectral indices is a further complicating factor, although not important for the prediction of total numbers within certain flux-density limits, etc. At a given luminosity, sources with low α will be seen to higher redshifts than those with high α, leading to a selection effect favouring low α. Nevertheless, to first order, the total numbers of sources obtained will be the same as that calculated using $\bar{\alpha}$; unless predictions of α distributions are required therefore, the spread in α may be ignored in constructing the RLF.

Hence we make the following assumptions about the spectra of the flat-spectrum and steep-spectrum sources;

(a) For the flat-spectrum sources we assume a value $\alpha = 0$. This choice is restrictive, since it implies that all flat-spectrum source counts at all frequencies should look the same. In the absence of any evidence for a dependence of α on luminosity for these sources, this is nevertheless the best procedure we can adopt; indeed, if satisfactory models can be found for the flat-spectrum sources at several frequencies, then no more complex procedure is justified.

(b) For the steep-spectrum sources we assume a P–α correlation. This correlation was investigated most recently by Laing & Peacock (1980), who demonstrated that it was a feature only of the powerful extended sources. We should note at this point that, in fact, α correlates equally well with redshift. The assumption that the fundamental correlation is with luminosity is one that cannot be tested with the presently-available data. In view of the

lack of evolution of the low-luminosity sources, it seems implausible that their spectra should change with redshift, and we therefore regard it as more likely that α is physically correlated with luminosity (see Laing & Peacock 1980). This correlation is not an artefact, as it is in the opposite sense to the selection effects (see above). However, the correlation we wish to use in the models is the true relation, not the modified one which we observe in any flux-density-limited sample. This requires the selection effects to be quantified, which can only be done if the RLF is known. Laing & Peacock considered samples defined at 178 and 2700 MHz, whereas the best evolution models we have are those of WPL, defined at 408 MHz. It is thus necessary to re-analyse the P–α correlation for a sample selected at 408 MHz. This may be done using a subset of the 178-MHz sample considered by Laing & Peacock. This sample was selected to have $S_{178} > 10$ Jy and must therefore contain all sources

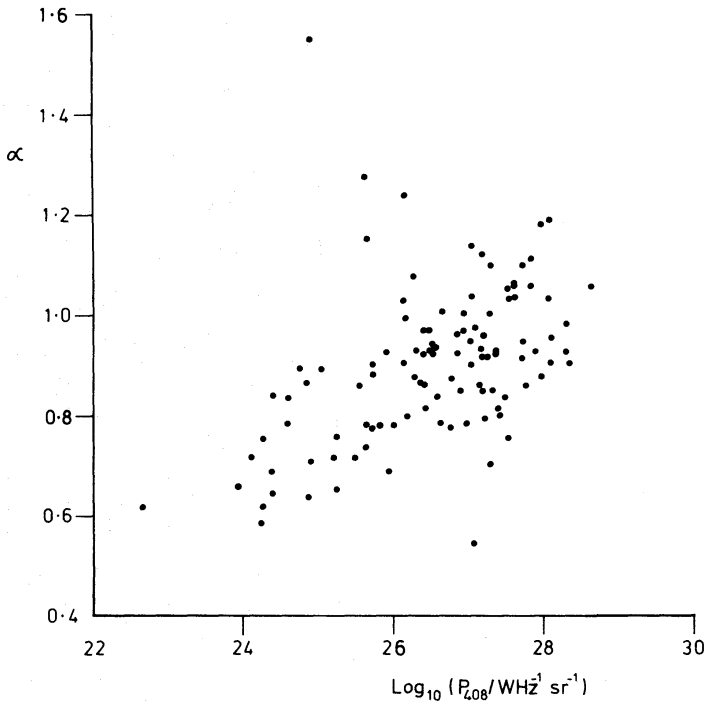

Figure 1. A plot of spectral index against 408-MHz luminosity for those sources in the 178-MHz sample of Laing & Peacock (1980) with $S_{408} > 6$ Jy.

in that area of sky with $S_{408} > 6$ Jy, since no extended source in the 178-MHz sample has $\alpha < 0.5$. Using that sample and the data from Laing & Peacock, we plotted α against P_{408} for the extended sources in a 408-MHz sample, as is shown in Fig. 1. The best-fitting line to this diagram is

$$\alpha = 0.065 \log_{10}(P_{408}) - 0.87 .$$

The rms deviation of the points in Fig. 1 from the fitted line yields a value $\sigma = 0.14$ for the spread in α, which does not vary greatly with luminosity. It is of course this scatter which is responsible for the selection effects that make the observed correlation differ from the true one. From a knowledge of σ, we can now calculate the magnitude of these selection effects. Consider the luminosity distribution $N(P)$ predicted by one of the WPL models on the assumption that all sources have a spectral index α. $N(P)$ is thus also a function of the value of α assumed. Now, if we assume α to have a mean $\bar{\alpha}$ and a variance σ^2, uncorrelated with

luminosity, the expectation value of α as a function of luminosity in the flux-limited sample is

$$\langle\alpha\rangle = \bar{\alpha} - k(P, \bar{\alpha}) \cdot \sigma^2,$$

where

$$k(P, \alpha) = \frac{1}{N(P, \alpha)} \cdot \frac{\partial N(P, \alpha)}{\partial \alpha}.$$

One of the WPL models may now be used to predict the P–α correlation, using WPL's assumption that $\bar{\alpha} = 0.75$. The result of this calculation is shown in Fig. 2, which was based on WPL model 5. Over the region in which the observed P–α correlation is best defined, the

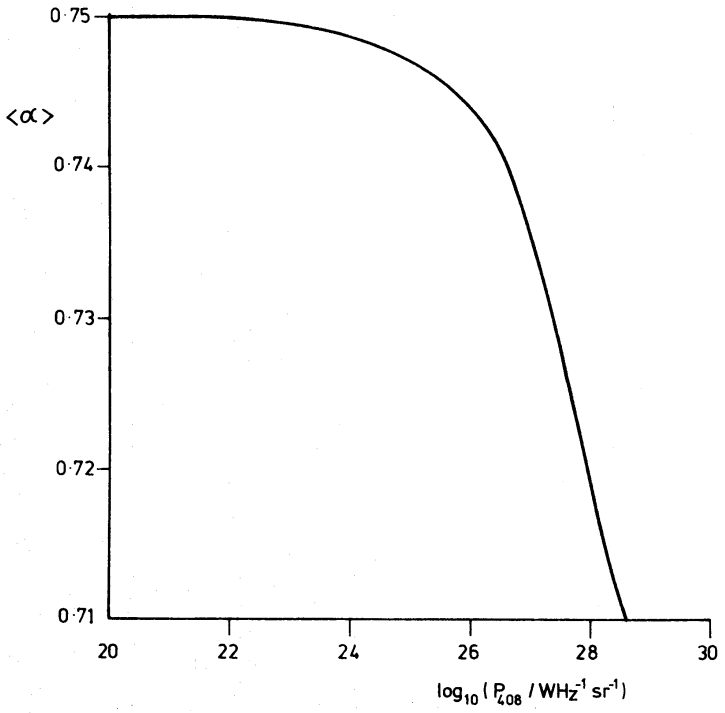

Figure 2. The P–α relation predicted by WPL model 5 if spectral index is uncorrelated with luminosity, and has a mean $\bar{\alpha} = 0.75$ and a spread $\sigma = 0.14$.

curve in Fig. 2 is approximately linear, with slope 0.015. So, to first order, the corrected value of the slope of the P–α relation is given by $0.065 + 0.015 = 0.08$. For the lowest-luminosity sources, extrapolation of the correlation yields very low values of α, which we know is not the case: Colla *et al.* (1975) find $\bar{\alpha} = 0.75$ for a sample of steep-spectrum, low-luminosity galaxies. We therefore split our assumed P–α relation for the steep-spectrum sources into two parts:

(a) $P_{408} < 10^{25}\,\mathrm{W\,Hz^{-1}\,sr^{-1}}$, $\alpha = 0.75$,

(b) $P_{408} > 10^{25}\,\mathrm{W\,Hz^{-1}\,sr^{-1}}$, $\alpha = 0.75 + 0.08\,(\log_{10}(P_{408}) - 25)$.

This completes the spectral framework that we shall use to make predictions from models for the RLF.

4 Free-form optimization

The methods for obtaining model RLFs used in the past suffer from the defect that the RLF produced reflects mainly the model builders' preconceived ideas as to its form, and yields little information on the range of evolution allowed by the data. Also, the models obtained can become unrealistic when it is necessary to assume extreme values of the assumed parameters to obtain a satisfactory fit. For example, the model by Robertson (1978) had an RLF which was discontinuous (a single 'switch-on' luminosity was assumed), model 4a of WPL was virtually discontinuous (a very narrow range of transition luminosities was required), and the model by Grueff & Vigotti suffered from similar defects. Moreover, as the observational data improve, it becomes harder to think of *ad hoc* forms for the RLF which may be adjusted to give results consistent with the observations. Robertson's approach overcame this problem to some extent, but was only a one-dimensional procedure; we require a free-form solution in two dimensions.

At present, the data are incomplete, so that the RLF cannot be obtained in a truly free-form manner; to progress, we are therefore forced to make *some* general assumptions about the solution. The simplest criterion is to require that the RLF be a smooth function of P and z, so that any large-scale features of the RLF will be reproduced by the model, but it is not easy to make such a smoothness criterion precise. Consider ρ_0 for example; where this is known directly it is approximately a power law in P, suggesting that $\log(\rho)$ should be in general a smooth function of $\log(P)$. The relevant frame in redshift is harder to define; to gain some feeling for the problem, we consider some of the evolution functions used in previous studies. The two major forms used have been $E \propto (1+z)^n$ and $E \propto \exp(m\tau)$; a third form used mainly on quasar data, $E \propto V^\beta$, where V is the volume corresponding to the distance at which the source lies, cannot be suitable for all types of source since it corresponds to a zero local density for any source which evolves at all, whereas there is evidence that the RLF is constant out to $z \simeq 0.2$ and evolves thereafter (Meier *et al.* 1979; Katgert, de Ruiter & van der Laan 1979).

Thus, two frames in which we might expect ρ to be smooth are $\log(P)$–$\log(1+z)$ and $\log(P)$–τ. Other frames could well be considered, although to encompass the observed facts of little evolution out to $z = 0.2$ and strong evolution by $z = 3$, they cannot differ radically from the two alternatives given above. For simplicity, therefore, we consider only these two cases; the two redshift frames are sufficiently different (especially at high z) to demonstrate to what extent the derived RLFs depend on the frame considered. It should be noted that the assumption that the RLF is smooth may not be correct at high redshifts, for it seems probable that the epoch of galaxy formation lies at redshifts in the range 3–10 (see e.g. Rees 1978), and in any case almost certainly occurs at redshifts less than 100. This process may well correspond to a 'switching-on' of radio sources over time-scales much shorter than their subsequent lifetimes. For this reason (and out of a desire to explore the full range of acceptable models), we have also constructed models that have a redshift cut-off – assuming the RLF to be smooth out to some critical redshift and zero thereafter. For simplicity, this redshift was taken to be the same for both steep-spectrum and flat-spectrum sources.

Having chosen the relevant coordinates, the simplest way of ensuring that ρ is a smooth function is to express it as a series expansion. The actual number of terms used in the expansion should be as small as possible, consistent with obtaining a satisfactory fit to the data; in practice, expansions of quartic order (15 coefficients) and cubic order (10 coefficients) were needed for the steep-spectrum and flat-spectrum RLFs respectively. The basis functions chosen to perform this expansion could be almost any set of orthogonal functions; the choice of a particular set is not important, since much larger changes will be made to the models by choosing a different set of coordinates in which to require the RLF to be smooth.

In practice, we chose to expand ρ as a power series: this has the advantage that the expansions for ρ_0 and E may be obtained immediately by separating out all the zero-order redshift terms. We therefore need to consider the following forms for ρ:

$$\log(\rho) = \sum_{i=0}^{n} \sum_{j=0}^{n-i} A_{ij} [\log P]^i [\log(1+z)]^j$$

or

$$\log(\rho) = \sum_{i=0}^{n} \sum_{j=0}^{n-i} B_{ij} [\log P]^i [\tau]^j ,$$

and adjust the parameters A_{ij} or B_{ij} so that the fit of the model to the data is optimized. To do this, we require a measure of the fit of the model to the data; we take this to be simply the total value of χ^2, summed over all the data. This simple criterion is unsatisfactory in that it may lead to solutions in which one set of data is fitted extremely well at the expense of others, whereas an acceptable solution should have a reasonable fit for all data sets. This may be achieved in practice by giving added weight to the badly-fitted data sets until a satisfactory fit over the whole of the data is achieved. Although crude, this procedure is not completely subjective: it is merely a way of remedying the defects in the solution caused by the adoption of the simple χ^2 criterion.

To optimize the expansion coefficients, we take an initial guess for the coefficients – yielding a value for χ^2 of χ_0^2 – and alter the coefficients iteratively so as to reduce χ^2. This was done via a simple second-order Taylor expansion of χ^2:

$$\chi^2 \simeq \chi_0^2 + \mathbf{G} \cdot d\mathbf{A} + \frac{1}{2} d\mathbf{A} \cdot \boldsymbol{H} \cdot d\mathbf{A} ,$$

where $\mathbf{A}$ is a vector whose elements are the expansion parameters, $\mathbf{G}$ is the vector whose elements are the derivatives of χ^2 with respect to the parameters in $\mathbf{A}$, and $\boldsymbol{H}$ is the Hessian matrix of second derivatives of χ^2 with respect to the parameters in $\mathbf{A}$. To this order of approximation, the local minimum in χ^2 may be found by solving

$$\boldsymbol{H} \cdot d\mathbf{A} = -\mathbf{G} .$$

Both $\mathbf{G}$ and $\boldsymbol{H}$ may be found analytically for a given expansion, and the optimization proceeds iteratively by replacing $\mathbf{A}$ by $\mathbf{A} + d\mathbf{A}$. This scheme is simple in principle, but there are difficulties with its implementation. Far from the solution, the χ^2 hypersurface is unlikely to resemble the quadratic approximation very closely. The iterative scheme outlined above may thus give a step which is much too large – this was controlled by putting a limit on the changes made to $\mathbf{A}$ in any one iteration. Far from the solution, there is no guarantee that the curvature of the χ^2 hypersurface is everywhere concave – it is possible that saddle points may exist in the quadratic approximation. These are dealt with by testing the eigenvalues of the matrix $\boldsymbol{H}$: when a negative eigenvalue is found, the iteration will be moving towards the stationary value, i.e. towards the saddle point. If we separate out the component of $d\mathbf{A}$ in the direction of the eigenvector of $\boldsymbol{H}$ which corresponds to the negative eigenvalue, then subtracting that component from $\mathbf{A}$ moves us away from the saddle point. Also, if the χ^2 hypersurface is not everywhere concave, there is no guarantee that the final point which is found is unique – several local minima could exist. This possible variety of solutions within one model is not important, however, because we have considered the much larger range of variation inherent in different expansion forms. Finally, the iterative scheme is extremely expensive in computer time. For M expansion coefficients and a grid of side N, the number of operations needed to find H is $\sim M^2N^2$ – which, for quartic-order expansions ($M = 15$ for

each spectral type) and $N = 100$, corresponds to 10^7 operations per iteration. This means in practice that several hours CPU time are required for a solution of the problem. The calculations were performed on a VAX 11/780.

5 Observational constraints

The data which are relevant to the problem of constructing the RLF divide into four main groups: (i) the local RLF; (ii) source counts; (iii) luminosity/redshift distributions, and (iv) V/V_{max} tests.

5.1 THE LOCAL RLF

For weak sources ($P_{408} \lesssim 10^{25}\,\mathrm{W\,Hz^{-1}\,sr^{-1}}$), the local RLF may be constructed by searching for optical identifications of faint radio sources to some limit of apparent magnitude. For the sources identified with bright galaxies, z is small enough so that $E = 1$ and ρ_0 may be found directly. For the flat-spectrum sources, ρ_0 may be derived from the data of Ekers & Ekers (1973) and Colla *et al.* (1975). This luminosity function is not very well defined, but suffices to constrain the low-luminosity end of the flat-spectrum RLF. We note that the points derived from the work of Ekers & Ekers and Colla *et al.* are consistent with each other.

A total local RLF at 408 MHz similar to that used by WPL may be constructed from the data of Cameron (1971), Caswell & Wills (1967) and Meier *et al.* (1979). From this, we may derive a local RLF for steep-spectrum sources, since Colla *et al.* (1975) have shown that $\rho_{steep}/\rho_{flat} \simeq 30$ for $P_{408} \lesssim 10^{21.5}\,\mathrm{W\,Hz^{-1}\,sr^{-1}}$ and $\rho_{steep}/\rho_{flat} \simeq 5$ for greater luminosities. Since the contribution of flat-spectrum sources to the total at this frequency is small, the derived steep-spectrum local RLF should be accurate. Finally, this function was translated to 2700 MHz using $\alpha = 0.75$ (see Section 3). These two local RLFs are shown in Fig. 3, together with the predictions of model 1 (see Section 6.1).

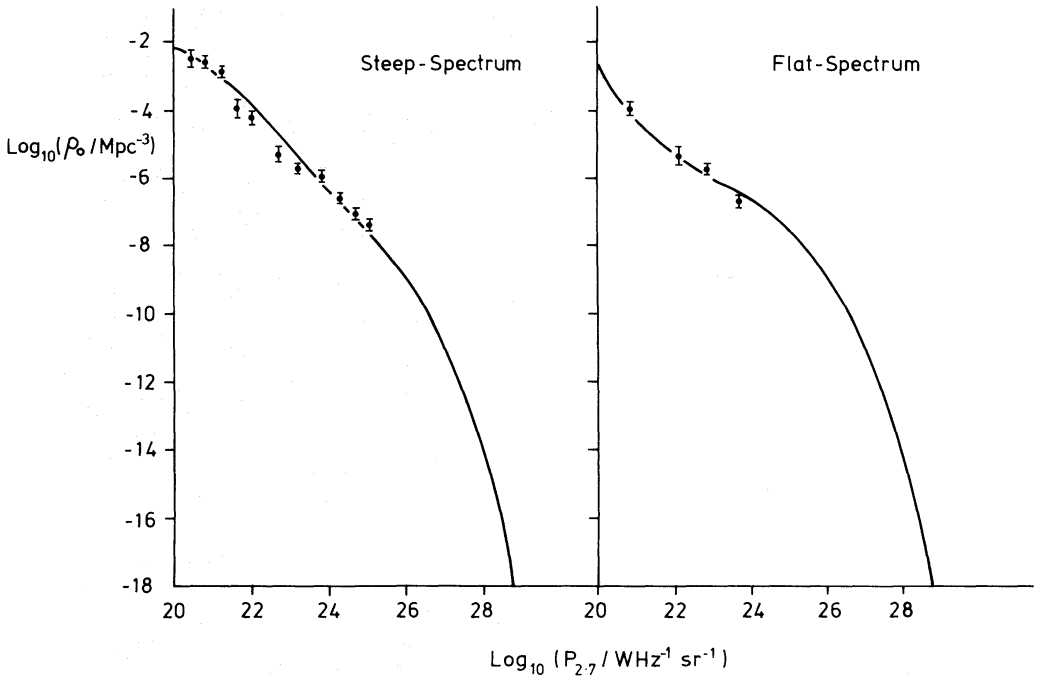

Figure 3. The data on the local RLF, together with the predictions of model 1.

5.2 SOURCE COUNTS

We have considered source counts at four frequencies: 5000, 2700, 1400 and 408 MHz. Both the 5000-MHz counts (from the NRAO/Bonn surveys; Kellermann 1980) and the 2700-MHz counts (from the Parkes surveys; Wall *et al.* 1981) are available in spectrally separated form. The 5000-MHz counts have recently become much better defined, to the extent that the turnover of the count for the flat-spectrum sources at low flux densities is now seen. Spectrally separated counts at 1400 MHz are available at two flux-density levels only (2 Jy and 10 mJy), from the NRAO survey (Bridle *et al.* 1972) and the Cambridge 5C surveys (Pearson & Kus 1978).

At 408 MHz, only the total count is available – although it is the best-defined of all the source counts considered here. This is based on the All-Sky catalogue of Robertson (1973), the B2 survey (Colla *et al.* 1973) and the 5C5, 5C6 and 5C7 surveys (Pearson & Kus 1978). Additionally, there is the determination of the total count at 2700 MHz at mJy levels using a $P(D)$ analysis (Wall & Cooke 1975).

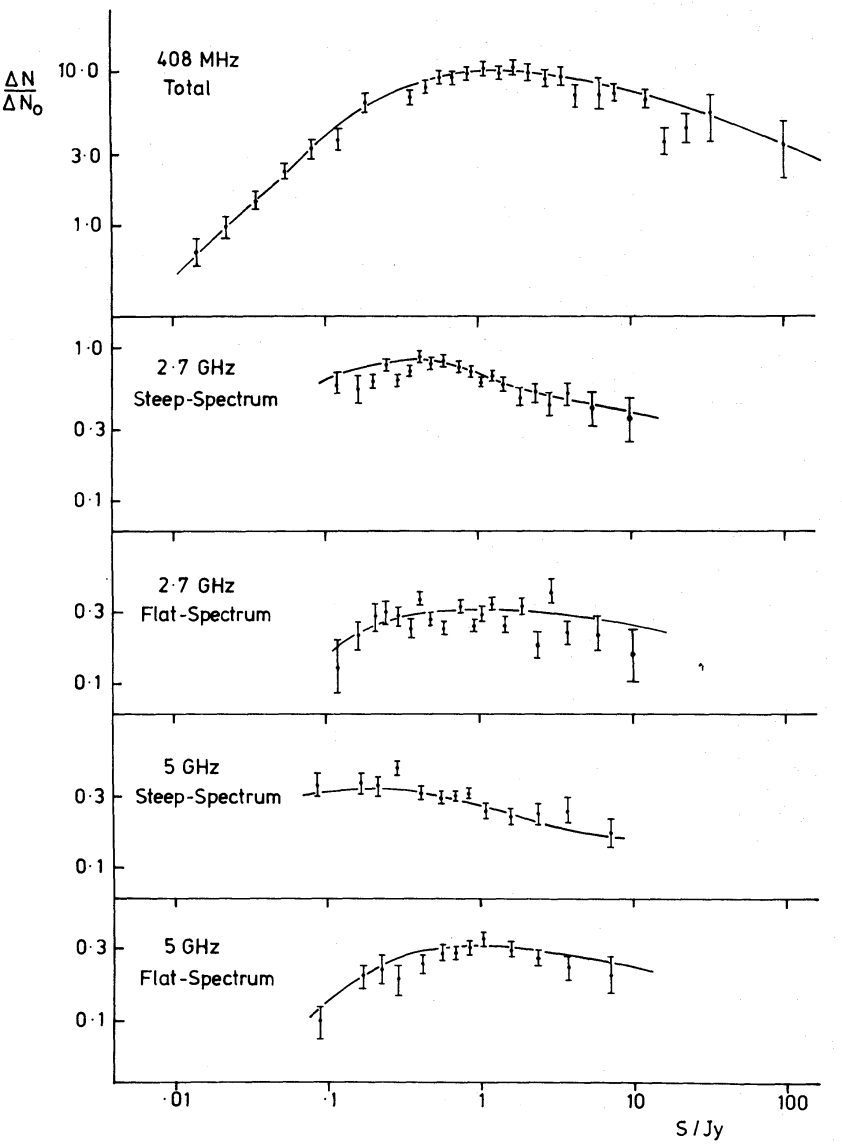

Figure 4. The source-count data at 408, 2700 and 5000 MHz, together with the predictions of model 1. All counts are normalized to the Euclidean prediction $N_0 = 100\ (S/Jy)^{-1.5}$.

The source counts at 408 MHz, 2.7 and 5 GHz are shown in Fig. 4 together with the predictions of model 1.

5.3 LUMINOSITY/REDSHIFT DISTRIBUTIONS

As was discussed in Section 1, the luminosity data from bright-source samples are of crucial importance in interpreting the source-count data. Recent programmes of deep optical identifications (Gunn *et al.* 1981; Peacock *et al.* 1981) have provided improved luminosity information for samples of sources selected at 178 MHz (the 166-source sample of Jenkins, Pooley & Riley 1977) and at 2700 MHz (the 168-source sample of Peacock & Wall 1981). In effect, the former sample provides data on the steep-spectrum sources only, whereas the latter sample provides also crucial data on the flat-spectrum sources. Due to the P–α correlation, the 178-MHz sample contains a higher proportion of powerful steep-spectrum sources than does the 2700-MHz sample, confirming that a realistic model must take account of this correlation (see Section 3). These luminosity distributions are shown in Fig. 5, together with the predictions of model 1.

Because of the difficulty of identifying faint sources, luminosity distributions for deeper samples are incomplete, but useful information may still be obtained. We have considered two further data sets:

(a) The sample complete to 0.9 Jy at 408 MHz used by Grueff & Vigotti (1977) in their evolution model.

(b) The identification statistics for the 5C6 and 5C7 surveys reported by Perryman (1979a, b).

Grueff & Vigotti's 0.9-Jy sample contained 526 sources, of which 63 per cent (40 per cent galaxies and 23 per cent quasars) could be identified to a limiting visual magnitude of

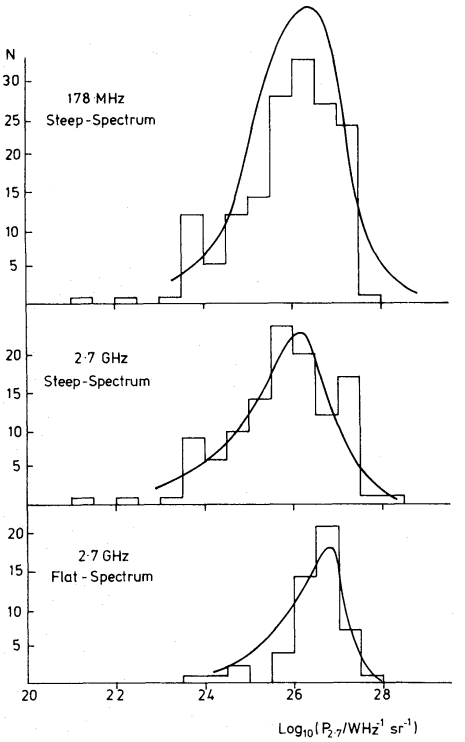

Figure 5. The luminosity distributions for bright-source samples selected at 178 MHz and 2.7 GHz, together with the predictions of model 1.

22.5. The redshift information is minimal but, for the galaxies, redshifts can be estimated from an m–z plot, thus providing the redshift distribution for galaxies out to about $z = 0.8$. However, unlike Grueff & Vigotti, we need a redshift distribution for the whole sample – so we also need an estimate of the quasar redshift distribution. This may be obtained from the data of Wills & Lynds (1978), who considered a sample of quasars with $S > 2$ Jy at 178 MHz – a limit similar to that of Grueff & Vigotti. By assuming (i) that these two quasar redshift distributions have similar shapes, and (ii) that Grueff & Vigotti have identified all the quasars in their sample, we obtain an estimate of the total redshift distribution for this sample, out to $z = 0.8$. The contribution to this distribution from quasars is small, so inaccuracies in this procedure are not important; more worrying is the fact that so many of the galaxy redshifts are estimated values. Because of these uncertainties, we produced a redshift distribution with only three bins. This is the least satisfactory data set employed in this study, but it must be incorporated, since it contains the best identification data available at intermediate flux densities. In practice, models consistent with this data set could be found.

Finally, we used the work of Perryman (1979a, b), who sought identifications for the 5C6 and 5C7 surveys on plates with a limiting visual magnitude of 22. The result was that 77 out of 428 sources detected at 408 MHz were identified (after allowing for background contamination). The flux-density limit of these surveys was about 10 mJy at 408 MHz but, since the area of the survey was a function of the limiting flux density, the 5C samples do not constitute a simple flux-density limited sample. From a knowledge of the variation of area for different flux-density limits (Pearson & Kus 1978), the effective limiting flux density was found to be about 22 mJy. If we assume that most sources at such low flux densities will be galaxies, then we can obtain an estimate of the redshift distribution for these samples once the redshift corresponding to the $V = 22$ mag limit is known. For bright radio galaxies, $V = 22$ mag would correspond to $z \simeq 1.0$ but, since we may be dealing with weak radio galaxies, the absolute magnitudes involved could be fainter than for the giant ellipticals associated with the more powerful sources. Gunn (1978) gives the absolute magnitude of such giant ellipticals as $\langle M \rangle = -22.5$, whereas Colla *et al.* (1975) find $\langle M \rangle = -21.5$ for their sample of weak radio galaxies. The limiting redshift corresponding to $V = 22$ mag for the 5C samples is therefore probably about 0.6. Although this is a very rough estimate, models consistent with it could be found.

5.4 $V/V_{\rm max}$ TESTS

The final body of information which relates to the problem of cosmological evolution comprises the results of the various $V/V_{\rm max}$ tests. Each of these produces simply one number, $\langle V/V_{\rm max} \rangle$, which is related to how steeply the RLF is increasing with redshift. The results of this test are determined principally by the slope of the source counts and are fairly insensitive to the redshifts assigned to each source (see e.g. Longair & Scheuer 1970). For this reason, it was not originally thought necessary to include the results of the $V/V_{\rm max}$ tests in this study. Preliminary results nevertheless revealed a range of models, all consistent with the source counts and luminosity distributions, but with significantly different $\langle V/V_{\rm max} \rangle$ values. The problem was that simply dividing the source-count data into separate bins as we have done is not the optimum way of constraining the slope of the counts. On the other hand, the $V/V_{\rm max}$ test makes use of all the data above a limiting flux density to produce essentially a best estimate of the slope of the source counts at that point.

The difficulty with $V/V_{\rm max}$ tests is that the vast majority of them have been based on samples of quasars only. This will closely approximate the whole population for the flat-spectrum sources (see e.g. Peacock & Wall 1981), but not for the steep-spectrum sources.

The results we considered were those of Wills & Lynds (1978) and Masson & Wall (1977), who used samples of flat-spectrum quasars selected at 2700 MHz by the criterion $S > 0.35$ Jy, and those of Peacock *et al.* (1981) who evaluated V/V_{max} for the 168-source sample of Peacock & Wall (1981), for which $S_{2.7} > 1.5$ Jy. For flat-spectrum quasars, the results of Masson & Wall and Wills & Lynds suggest a value of $\langle V/V_{max} \rangle = 0.58 \pm 0.05$ at 0.35 Jy, whereas Peacock *et al.* found $\langle V/V_{max} \rangle = 0.675 \pm 0.038$ at 1.5 Jy. For the steep-spectrum sources, Peacock *et al.* found $\langle V/V_{max} \rangle = 0.661 \pm 0.036$ for the powerful sources ($P_{2.7} > 10^{26}$ W Hz^{-1} sr^{-1}), and $\langle V/V_{max} \rangle = 0.536 \pm 0.035$ for sources weaker than this. This change of $\langle V/V_{max} \rangle$ with flux-density limit for the flat-spectrum sources, and the differential evolution for the steep-spectrum sources are in good agreement with the form of the source counts.

6 Results

6.1 SUCCESSFUL MODELS

Despite the wide range of data considered in Section 5, the iterative procedure was able to find models which made predictions in satisfactory agreement with the observations. On the whole, no evidence was found for inconsistencies in the data, but there was one exception – the luminosity distribution for the 178-MHz sample. The shape of the distribution could be reproduced, but the total number of sources predicted was incorrect: in the area of sky where 166 sources were observed, about 230 were predicted. At this stage, no corrections had been made for possible errors in the flux-density scales; for the majority of the data considered, these cannot be in error by more than a few per cent. At 178 MHz, however, the scale used to define the sample (that of Kellermann, Pauliny-Toth & Williams 1969) is drastically too low, and correction factors of between 1.09 (Roger, Bridle & Costain 1973) and 1.225 (Wills 1973) have been suggested. In their study of spectral curvature, Laing & Peacock (1980) found that the assumption of a scaling factor of 1.09 led to 178-MHz flux densities still low by an average of 15 per cent when compared to a power-law extrapolation from higher frequencies. Because of this, the simple assumptions of power-law spectra used in the present study will yield 178-MHz flux densities which are higher than those used in the 178-MHz sample by about 28 per cent. This resolves the discrepancy: if the model is required to predict a luminosity distribution at 178 MHz for a sample with $S_{178} > 12.8$ Jy rather than 10.0 Jy, then a luminosity distribution consistent in size and shape with the observed one is predicted. There is nevertheless a limit to the lowest frequencies at which the model can make useful predictions. At 178 MHz, it is not clear to what extent the discrepancy between observed and extrapolated flux densities is due to curvature of the spectra or to a poor flux-density scale. At lower frequencies, on the other hand, it is certain that strong spectral curvature does exist. In view of this, and the lack of reliable 178-MHz flux densities, the models are not expected to provide quantitatively correct predictions for frequencies below 408 MHz.

After this one adjustment, it was possible to produce models which were consistent with all the data. Quartic-order and cubic-order expansions were required for the steep-spectrum and flat-spectrum sources respectively. For the expansions in both $\log(1+z)$ and τ, values of χ^2 in the range 220–250 were obtained for the 151 data-bins. From a formal point of view, these values are high, but in view of the systematic errors which must exist (due to different flux density scales, estimated redshifts, etc.), the models should not be rejected. In fact, the fit to the individual data sets is always acceptable (*cf.* Figs 3, 4 and 5). When models possessing an assumed redshift cut-off were investigated, fits as good as those above could be found for cut-off redshifts greater than 10. For smaller values of the cut-off redshift, the best fit was generally poorer, with χ^2 reaching values around 350 for a cut-off at $z = 3$. This rise is not

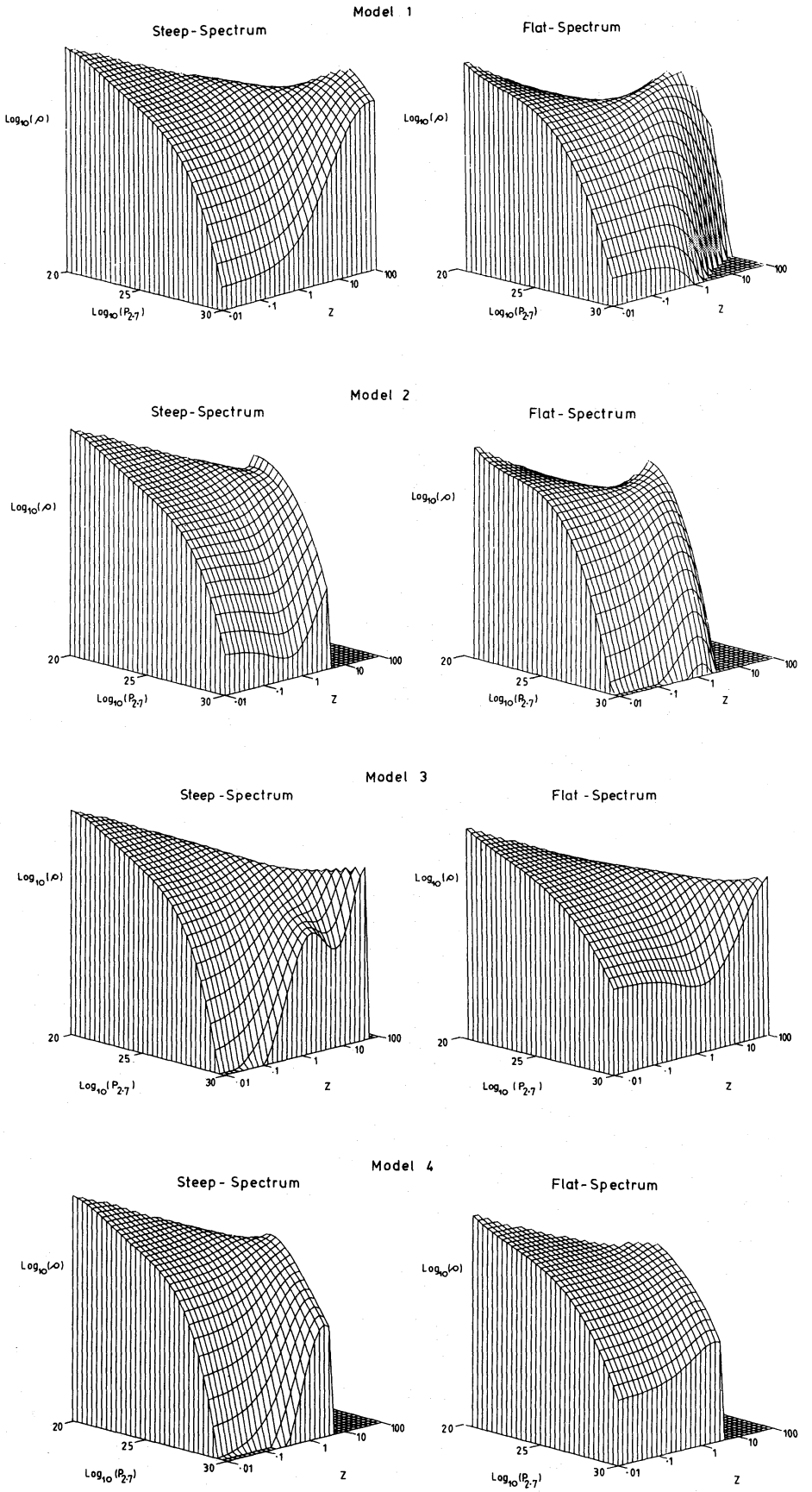

Figure 6. Perspective plots of the steep-spectrum and flat-spectrum RLFs for models 1–4. The vertical scale is the same in each case (see Fig. 3).

due to any one data set, but to a degradation of the overall fit. Models with a cut-off at $z = 5$ still produced reasonable fits.

In presenting these results in detail, we concentrate on only four models: the expansions in $\log(1+z)$ with and without a cut-off at $z = 5$ for $q_0 = 0.5$ and $q_0 = 0$. We number these as follows: model 1 – no cut-off, $q_0 = 0.5$; model 2 – cut-off at $z = 5$, $q_0 = 0.5$; model 3 – no cut-off, $q_0 = 0$; model 4 – cut-off at $z = 5$, $q_0 = 0$. The optimized expansion coefficients for these models are given in the Appendix, and Fig. 6 displays separate perspective plots of the steep-spectrum and flat-spectrum RLFs. It is clear from Fig. 6 that considerable variations exist between the models, particularly in the regions of high luminosity and high redshift. No reliance should be placed upon features seen in these latter regions, since the RLF is not well-defined there (see Section 6.2) and the predicted contributions to observed data from these areas are usually small. Nevertheless, the general features of these RLFs are similar, and for both spectral types there is strong evolution for the most powerful sources. For the flat-spectrum sources this is in apparent conflict with earlier statements, and we return to this point in Section 6.3. With the partial exception of the flat-spectrum RLFs in models 1 and 2, we see that there is no overall tendency for the RLFs to decrease at high redshifts. Although the data are consistent with the presence of a redshift cut-off, it therefore seems that there is no strong evidence for the reality of such an effect. To indicate the degree of success of each model, Table 1 shows the values of χ^2 for each data set, for each of these four models; in general, the fit is superior for models in the $q_0 = 0.5$ Universe. The only set of data with an unacceptable fit is the steep-spectrum local RLF, but this data set is used only to fix the low-luminosity end of the RLF and has no bearing on the evolutionary behaviour of the more luminous sources; it is not worth increasing the expansion order merely to fit this one data set.

Table 1. Comparison between models and data.

Data set	Number of bins	Values of Chi-squared: Without z cut-off q_0=0.5	Without z cut-off q_0=0	With z cut-off q_0=0.5	With z cut-off q_0=0
2700 MHz steep-spectrum luminosity distribution	10	15.1	13.5	15.4	16.0
2700 MHz flat-spectrum luminosity distribution	10	14.2	15.4	14.6	23.3
178 MHz steep-spectrum luminosity distribution	10	16.2	16.2	13.3	15.2
5000 MHz steep-spectrum source count	13	22.6	25.4	18.4	25.8
5000 MHz flat-spectrum source count	13	10.6	12.2	7.6	16.2
2700 MHz steep-spectrum source count	20	33.4	39.3	33.4	40.2
2700 MHz flat-spectrum source count	20	18.6	25.0	20.4	24.4
2700 MHz P(D) total source count	1	0.1	1.0	0.1	0.1
1400 MHz steep-spectrum source count	2	2.7	2.0	3.2	6.1
1400 MHz flat-spectrum source count	2	0.5	0.4	0.6	0.3
408 MHz total source count	27	36.5	41.0	39.7	46.6
2700 MHz steep-spectrum local RLF	11	37.6	39.6	34.4	31.3
2700 MHz flat-spectrum local RLF	4	3.0	2.3	4.4	2.3
408 MHz 5C identification statistics	1	0.1	0.1	0.1	0.2
408 MHz 0.9-Jy redshift distribution	3	4.0	2.1	2.9	1.4
2700 MHz V/Vmax data	4	9.0	9.1	9.1	10.6
Total	151	224.2	244.6	217.6	260.0

6.2 VARIATIONS BETWEEN MODELS

Having produced successful models of the RLF, we now wish to investigate the degree of variation allowed by the data. One way of doing this would be to put formal error bars on each of the expansion coefficients, and thereby find the variations allowed to a given model, but model-independent answers are of greater interest. It is therefore much more useful to consider the variations between models of different kinds. For each value of q_0, we have three models – the quartic/cubic expansions in $\log(1+z)$ and τ, and also the expansions in $\log(1+z)$ with a redshift cut-off. To these we may add the cubic/cubic expansions in $\log(1+z)$ and τ (these provide nearly as good a fit to the data as do the quartic/cubic models, although not quite good enough to be acceptable). We may expect these five models to indicate the range of variation allowed for smooth models by the data. The simplest way

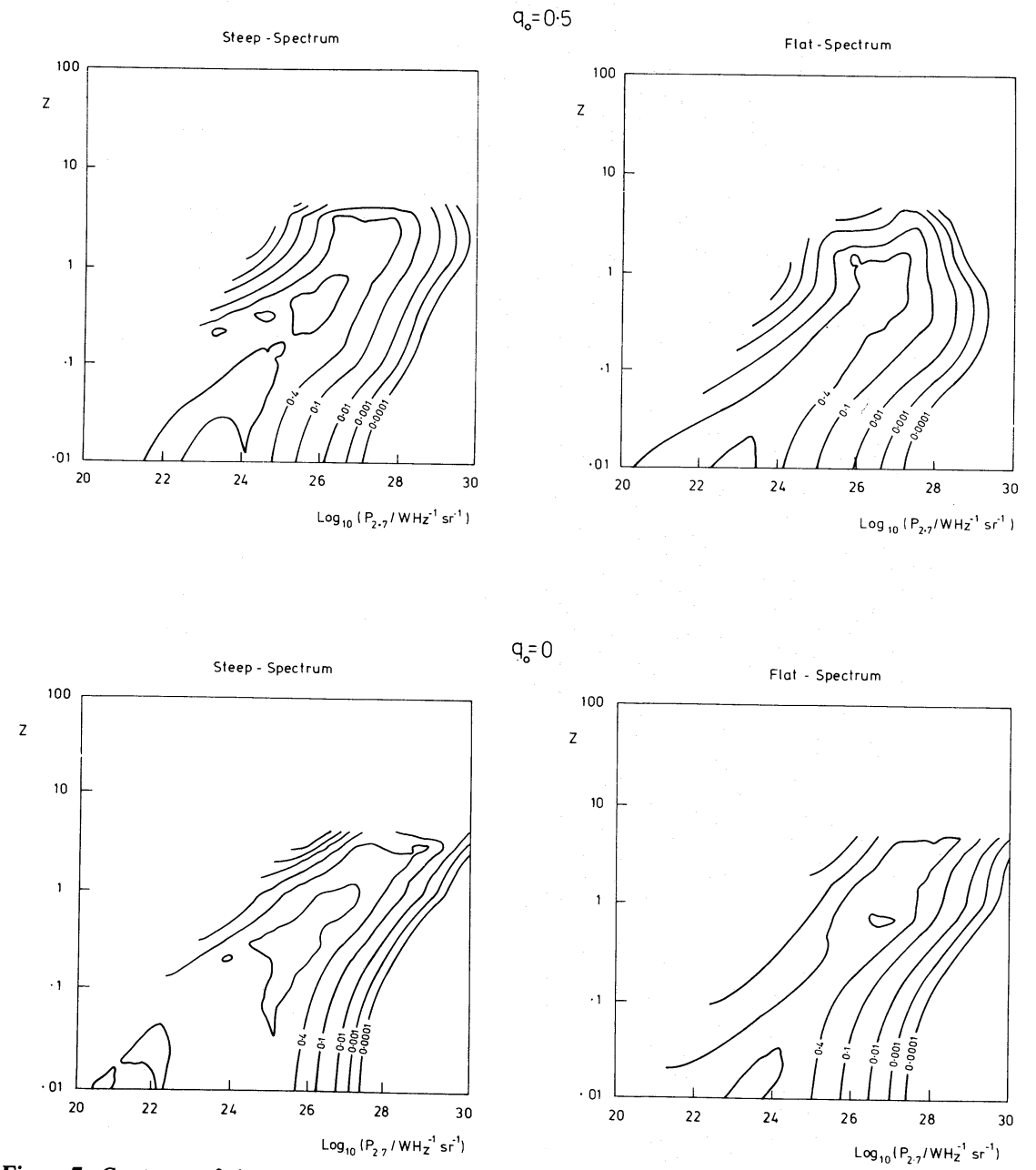

Figure 7. Contours of the parameter R over the P–z plane for $q_0 = 0.5$ and $q_0 = 0$. Contours are plotted at $R = 0.8, 0.4, 0.1, 0.01, 0.001, 0.0001$.

to discover from these results the degree to which the RLF is constrained is to consider the variation of ρ from model to model. We define a reliability parameter, R, to be the ratio of the smallest model value of ρ to the largest value at a given point on the P–z plane. Where this parameter is close to 1, the RLF is well defined; but where R is less than (say) 0.1, the RLF is not strongly constrained by the data. Fig. 7 shows contour plots of R over the P–z plane, for the two geometries considered. We see that the RLF is only well-defined ($R > 0.1$) in a strip that lies along a line of constant flux density, corresponding to the limit of the bright-source samples for which we have complete redshift information. Away from this strip, we see that even the large amounts of data used in this study are insufficient to specify the RLF closely.

At high flux densities, the uncertainty in the models is a fundamental one – there is only a comparatively small number of sources over the whole sky. The prospects for future improvements therefore lie at lower flux densities; if complete redshift information could be obtained for sources a factor of ~ 10 fainter than the present bright-source samples, this would probably suffice to extend the region of high R down to the lowest flux densities used here – about 10 mJy at 408 MHz. It is most important that such studies be carried out at high frequencies, so as to ensure adequate representation of the flat-spectrum sources. To indicate the power of redshift data for faint sources in resolving the uncertainties present in the evolution models, Fig. 8 shows the redshift distributions predicted by models 1–4 for a sample selected to have $S > 50$ mJy at 5 GHz. There are wide variations between these predictions, especially for the flat-spectrum sources, and good data on a sample of this sort would be invaluable. With the advent of solid-state optical detectors of high sensitivity and dynamic range, the task of identifying and measuring redshifts for very faint optical objects

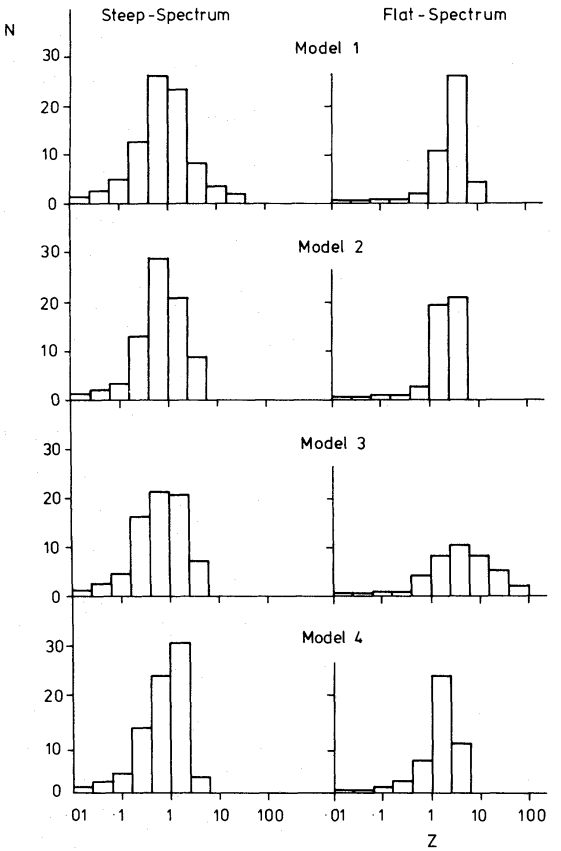

Figure 8. The redshift distributions predicted by models 1–4 for a sample of sources with $S > 50$ mJy at 5 GHz, over an area of 0.03 sr.

has been substantially eased, and the identification of a large sample of faint radio sources can now be regarded as a practical proposition. Furthermore, there is the prospect that such deep identifications might be easier of the flat-spectrum sources: Condon, Balonek & Jauncey (1976) identified a sample selected at 0.1 Jy at 2.7 GHz on the prints of the Palomar Sky Survey and found that it was possible to identify 64 per cent of the flat-spectrum sources in their sample, as opposed to only 40 per cent for the steep-spectrum sources.

6.3 THE EVOLUTION OF FLAT-SPECTRUM SOURCES

We have seen in Section 6.1 that the evolution models developed here yield similar results for both steep-spectrum and flat-spectrum sources, namely that sources of high luminosity show strong evolution. These similarities are particularly interesting in view of the differences in evolutionary behaviour previously ascribed to the steep-spectrum and flat-spectrum sources. In order to compare the evolutionary behaviours of the steep-spectrum and flat-spectrum sources more closely, we consider the evolution function $E(P, z)$. Contour plots of E are shown in Fig. 9 for models 1–4; only the areas within the $R = 0.1$ contours from Fig. 7 are included. These plots demonstrate the existence of close similarities between the predictions of all the models; both spectral types undergo differential evolution, the strength of evolution increasing with luminosity. For the steep-spectrum sources, all models predict that the numbers of weak sources remain essentially constant with cosmological epoch; the results for the flat-spectrum sources are similar, although models 1 and 2 predict some negative evolution for the weak sources. This may be due to the lack of good source counts for the flat-spectrum sources at the faintest flux densities; the data require differential evolution, but are not yet sufficiently well-defined to force the weak sources to have zero evolution. Similarities also exist in the strengths of evolution predicted by the models; for both spectral types, values of $E \simeq 100$ are achieved for sources with $P_{2.7} = 10^{27}\,\mathrm{W\,Hz^{-1}\,sr^{-1}}$ at a redshift of 1. This alone is sufficient to demonstrate that the high-luminosity flat-spectrum sources are undergoing strong cosmological evolution. The strengths of evolution at higher luminosities and redshifts are uncertain, since values of $E(P, z)$ in this area of the P–z plane refer to a local RLF which is not well defined. Nevertheless, the rates of evolution as inferred from the increase of $E(P, z)$ with redshift continue to be well-constrained within the $R = 0.1$ contours. There are differences between the behaviours of the two spectral types, with the evolution for the steep-spectrum sources apparently becoming faster than that for the flat-spectrum sources at higher redshifts. By the very nature of the spectra of the two classes of source, however, differences are certain to occur – if the functions $E(P, z)$ are the same for both spectral types at one frequency, they must differ at another. The point at issue is not so much whether the evolutionary histories of the two spectral classes are the same, but whether the flat-spectrum sources undergo strong evolution at all. The results of the present study indicate that they do, in apparent contradiction with the results of previous workers.

Previous statements attributing only weak evolution to the flat-spectrum sources were based almost exclusively on the results of V/V_{max} tests performed on samples of quasars selected at high frequencies (Schmidt 1968; Masson & Wall 1977; Wills & Lynds 1978). These workers obtained values of $\langle V/V_{\mathrm{max}} \rangle$ in the range 0.5–0.6 for their flat-spectrum quasars, whereas values of about 0.7 were found for steep-spectrum quasars; this was interpreted as implying a smaller degree of evolution for the flat-spectrum sources. The samples of flat-spectrum quasars used in these studies were generally selected at relatively low flux densities (0.6 Jy at 5 GHz or 0.35 Jy at 2.7 GHz); for brighter sources, however, different

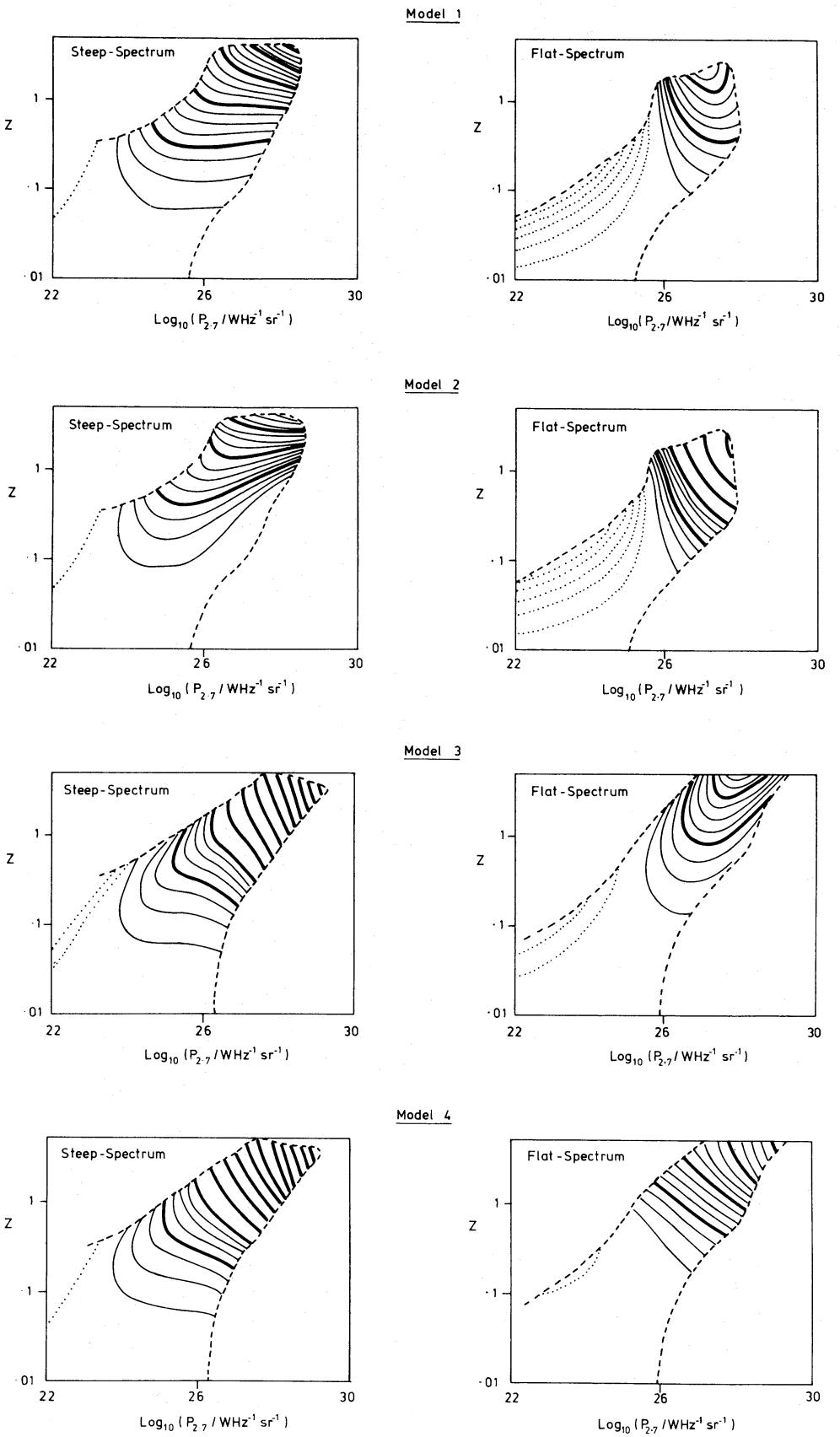

Figure 9. Contour plots of $E(P, z)$ within the $R = 0.1$ contours from Fig. 7, for models 1–4. Contours are plotted at equal intervals in $\log_{10}(E)$; the heavy contours represent $\log_{10}(E) = 1, 2, 3$ etc. and the light contours represent $\log_{10}(E) = 0.25, 0.5, 0.75$ etc. Negative contours are shown dotted.

results were obtained. Blake (1978) found $\langle V/V_{max}\rangle = 0.718 \pm 0.05$ for quasars with flat high-frequency spectral indices in the 1400-MHz catalogue of Bridle *et al.* (1972), for which $S_{1400} > 2$ Jy. Peacock *et al.* (1981) found $\langle V/V_{max}\rangle = 0.675 \pm 0.038$ for the flat-spectrum quasars in the 2.7-GHz sample of Peacock & Wall (1981), for which $S_{2700} > 1.5$ Jy. Peacock *et al.* (1981) pointed out that this change of $\langle V/V_{max}\rangle$ with flux density level is consistent with the form of the flat-spectrum source counts, which steepen at the highest flux densities. The low values of $\langle V/V_{max}\rangle$ obtained in early studies of flat-spectrum sources reflect the fact that, at 2.7 GHz or 5 GHz, the flat-spectrum source counts turn over at higher flux densities than do the steep-spectrum source counts. The results obtained at flux densities around 0.5 Jy thus refer to a region where the flat-spectrum counts have flattened, but the steep-spectrum counts are still steep – leading to a difference in the values of $\langle V/V_{max}\rangle$ obtained. In fact, the forms of the counts are not basically very different; at 1400 MHz, the turnovers of both counts occur at similar flux densities and the fraction of flat-spectrum sources then remains essentially constant between 2.0 Jy and 0.01 Jy (Pearson & Kus 1978).

The evolution of flat-spectrum sources was also investigated by Wall *et al.* (1981), who attempted to find evolution models which would fit the steep-spectrum and flat-spectrum source counts at 2.7 GHz. They considered exponential evolution (see Section 2) and concluded that the counts were best fitted by values of the parameter m in the range $10 < m < 12$ and $5 < m < 7$ for steep-spectrum and flat-spectrum sources respectively – thus apparently confirming the conclusions of the V/V_{max} test about the weaker evolution of flat-spectrum sources. However, this analysis did not allow differential evolution for the flat-spectrum sources; the models with high values of m therefore failed since they predicted far too many sources at low flux densities. In fact, the fits of exponential models with values of $m \simeq 10$ to the bright end of the flat-spectrum source counts were quite acceptable; it is therefore possible that the bright sources of either spectral type undergo similar degrees of evolution. The precise strengths of evolution appropriate for each spectral type are likely to remain in doubt, nevertheless, because the accuracy with which the slopes of the source counts are known is limited by the relatively small numbers of the brightest sources.

We therefore believe that the results of the present study are not inconsistent with those of previous workers. The low values of $\langle V/V_{max}\rangle$ obtained at lower flux densities are seen as being due to the different parts of the P–z plane which are sampled at different flux-density levels. This tendency for $\langle V/V_{max}\rangle$ to increase with flux density provides supporting evidence for the differential evolution of flat-spectrum sources predicted by our models. The question of the relative strengths of evolution of the flat-spectrum and steep-spectrum sources is not entirely settled by the current data, but these evolutionary strengths are certainly comparable in some areas of the P–z plane.

7 Conclusions

We have presented a new technique for deriving models for the cosmological evolution of extragalactic radio sources. By considering separate evolutionary histories for the steep-spectrum and flat-spectrum sources, and by using the P–α correlation for the steep-spectrum sources, consistency has been achieved between the models and source counts, luminosity distributions and identification data at all frequencies. The main conclusions from the present study of evolution models may be summarized as follows:

(1) The major features of previous models for the evolution of steep-spectrum sources have been confirmed: differential evolution with luminosity exists, and only the powerful sources exhibit large changes in their comoving densities with epoch.

(2) Differential evolution also exists for the flat-spectrum population, with the most powerful sources exhibiting evolution comparable in strength with that of the powerful steep-spectrum sources.

(3) The RLF is not so well-defined as had been supposed; in most areas of the P–z plane the present data do not suffice to define $\rho(P, z)$ to within a factor of 10. In particular, no conclusions can yet be drawn as to the presence/absence of a redshift cut-off.

(4) The most important future observational developments for resolving the uncertainties in the RLF will be (i) to obtain accurate source counts for faint flat-spectrum sources, and (ii) to obtain good identification and redshift data for samples of faint radio sources selected at high frequencies.

As further data become available, the models described in this paper will require modification, but the technique described here is sufficiently flexible to allow this to be done quite simply.

Acknowledgments

We thank Richard Ansorge, of the Cavendish High Energy Physics Group, for making available the computing facilities for this project. We also thank Irena Tabecka for producing the diagrams. Malcolm Longair, John Shakeshaft and Jasper Wall provided valuable comments on the presentation of this work. JAP thanks the SRC and the Cavendish Laboratory for financial support.

References

Blake, G. M., 1978. *Mon. Not. R. astr. Soc.*, **183**, 21P.
Bridle, A. H., Davis, M. M., Fomalont, E. B. & Lequeux, J., 1972. *Astr. J.*, **77**, 405.
Cameron, M. J., 1971. *Mon. Not. R. astr. Soc.*, **152**, 429.
Caswell, J. L. & Wills, D., 1967. *Mon. Not. R. astr. Soc.*, **135**, 231.
Colla, G., Fanti, C., Fanti, R., Ficarra, A., Formiggini, L., Gandolfi, E., Gioia, I., Lari, C., Marano, B., Padrielli, L. & Tomasi, P., 1973. *Astr. Astrophys. Suppl.*, **11**, 291.
Colla, G., Fanti, C., Fanti, R., Gioia, I., Lari, C., Lequeux, J., Lucas, R. & Ulrich, M.-H., 1975. *Astr. Astrophys.*, **38**, 209.
Condon, J. J., Balonek, T. J. & Jauncey, D. L., 1976. *Astr. J.*, **81**, 913.
Ekers, R. D. & Ekers, J. A., 1973. *Astr. Astrophys.*, **24**, 247.
Grueff, G. & Vigotti, M., 1977. *Astr. Astrophys.*, **54**, 475.
Gunn, J. E., 1978. In *Proc. Saas-Fee Summer School: Observational Cosmology*, Geneva Observatory, p. 65.
Gunn, J. E., Hoessel, J. G., Westphal, J. A., Perryman, M. A. C. & Longair, M. S., 1981. *Mon. Not. R. astr. Soc.*, **194**, 111.
Jenkins, C. J., Pooley, G. G. & Riley, J. M., 1977. *Mem. R. astr. Soc.*, **84**, 61.
Katgert, P., de Ruiter, H. R. & van der Laan, H., 1979. *Nature*, **280**, 20.
Kellermann, K. I., 1980. *Phys. Scripta*, **21**, 664.
Kellermann, K. I., Pauliny-Toth, I. I. K. & Williams, P. J. S., 1969. *Astrophys. J.*, **157**, 1.
Kulkarni, V. K., 1978. *Mon. Not. R. astr. Soc.*, **185**, 123.
Laing, R. A. & Peacock, J. A., 1980. *Mon. Not. R. astr. Soc.*, **190**, 903.
Longair, M. S., 1966. *Mon. Not. R. astr. Soc.*, **133**, 421.
Longair, M. S. & Scheuer, P. A. G., 1970. *Mon. Not. R. astr. Soc.*, **151**, 45.
Masson, C. R. & Wall, J. V., 1977. *Mon. Not. R. astr. Soc.*, **180**, 193.
Meier, D. L., Ulrich, M.-H., Fanti, R., Gioia, I. & Lari, C., 1979. *Astrophys. J.*, **229**, 25.
Peacock, J. A., Perryman, M. A. C., Longair, M. S., Gunn, J. E. & Westphal, J. A., 1981. *Mon. Not. R. astr. Soc.*, **194**, 601.
Peacock, J. A. & Wall, J. V., 1981. *Mon. Not. R. astr. Soc.*, **194**, 331.
Pearson, T. J. & Kus, A. J., 1978. *Mon. Not. R. astr. Soc.*, **182**, 273.

Perryman, M. A. C., 1979a. *Mon. Not. R. astr. Soc.*, **187**, 223.
Perryman, M. A. C., 1979b. *Mon. Not. R. astr. Soc.*, **187**, 683.
Rees, M. J., 1978. In *Proc. Saas-Fee Summer School: Observational Cosmology*, Geneva Observatory, p. 259.
Robertson, J. G., 1973. *Aust. J. Phys.*, **26**, 403.
Robertson, J. G., 1978. *Mon. Not. R. astr. Soc.*, **182**, 617.
Robsertson, J. G., 1980. *Mon. Not. R. astr. Soc.*, **190**, 143.
Roger, R. S., Bridle, A. H. & Costain, C. H., 1973. *Astr. J.*, **78**, 1030.
Schmidt, M., 1968. *Astrophys. J.*, **151**, 393.
Wall, J. V., 1975. *Observatory*, **95**, 196.
Wall, J. V., 1980. *Phil. Trans. R. Soc.*, **A296**, 367.
Wall, J. V. & Cooke, D. J., 1975. *Mon. Not. R. astr. Soc.*, **171**, 9.
Wall, J. V., Pearson, T. J. & Longair, M. S., 1980. *Mon. Not. R. astr. Soc.*, **193**, 683.
Wall, J. V., Pearson, T. J. & Longair, M. S., 1981. *Mon. Not. R. astr. Soc.*, **196**, 597.
Wills, B. J., 1973. *Astrophys. J.*, **180**, 335.
Wills, D. & Lynds, R., 1978. *Astrophys. J. Suppl.*, **36**, 317.

Appendix: Model expansion coefficients

This appendix gives the optimized expansion coefficients for models 1–4. We define the luminosity function $\rho(P, z)$ to be the number of sources per unit interval of $\log_{10}(P_{2.7})$ per Mpc^3 at redshift z. This choice of units means that the number of sources, N, in the small range of 2.7-GHz luminosities P_1 to P_2 and in the small redshift range z_1 to z_2 observed in an area A sr, is given by

$$N = \rho(P_1, z_1) \cdot \log_{10}(P_2/P_1) \cdot [V(z_2) - V(z_1)] \cdot \frac{A}{4\pi},$$

where $V(z)$ is the volume of space out to redshift z in Mpc^3 (assuming $H_0 = 50\,\mathrm{km\,s^{-1}\,Mpc^{-1}}$).

In models 1–4, we have expanded $\log_{10}(\rho)$ as a power series in $\log_{10}(P_{2.7})$ and $\log_{10}(1 + z)$. To do this, we define, for convenience, two coordinates x and y scaled so that they vary

Table A1. Model expansion coefficients for the steep-spectrum RLF.

Order of term		Expansion coefficient			
x	y	Model 1	Model 2	Model 3	Model 4
0	0	-2.09	-2.07	-2.12	-2.14
0	1	-46.13	-43.99	-90.79	-65.47
1	0	-0.79	-0.83	0.41	0.64
0	2	-52.41	-66.22	-353.22	-181.59
1	1	126.25	120.03	307.54	215.83
2	0	-13.09	-13.32	-17.17	-19.18
0	3	10.26	32.11	-218.62	-5.30
1	2	46.15	40.18	619.50	273.56
2	1	-95.21	-83.49	-315.94	-213.58
3	0	13.12	13.44	18.33	21.56
0	4	0.51	91.74	-44.56	13.16
1	3	-7.48	-115.92	198.06	-4.47
2	2	-8.17	35.03	-279.73	-105.63
3	1	22.91	12.85	107.08	70.30
4	0	-4.69	-4.65	-6.93	-8.32

Table A2. Model expansion coefficients for the flat-spectrum RLF.

Order of term		Expansion coefficient			
x	y	Model 1	Model 2	Model 3	Model 4
0	0	-2.04	-1.53	-2.68	-2.57
0	1	-108.22	-74.48	-46.83	-9.36
1	0	-11.69	-15.73	-7.75	-9.10
0	2	29.71	80.81	-34.34	22.78
1	1	150.02	76.54	78.43	4.70
2	0	12.45	19.96	5.13	7.92
0	3	-0.01	-0.18	-4.00	-5.28
1	2	-24.38	-66.05	25.28	-14.02
2	1	-48.82	-10.59	-30.54	2.95
3	0	-6.22	-10.10	-2.59	-3.99

by amounts of order unity over the P–z grid used here:

$x = (\log_{10}(P_{2.7}) - 20)/5$,

$y = \log_{10}(1 + z)$.

We now expand ρ as follows:

$$\log_{10}(\rho) = \sum_{i=0}^{n} \sum_{j=0}^{n-i} A_{ij} x^i y^j .$$

Thus, for each term in the expansion we must provide two coefficients, the values of A_{ij} appropriate for steep-spectrum and flat-spectrum sources. These values are given in Tables A1 and A2. Note that models 2 and 4 require the RLF to be set to zero beyond a redshift $z = 5$.